THE JOURNAL OF NAVIGATION (2007), **60**, 69–81. © The Royal Institute of Navigation
doi:10.1017/S0373463307004006 Printed in the United Kingdom

Mapping and Survey of Plasma Bubbles over Brazilian Territory

L. F. C. de Rezende, E. R. de Paula and I. J. Kantor,

(*National Institute for Space Research*, *São José dos Campos*, *SP Brazil*)
(Email: luizfelipe@dae.inpe.br)

P. M. Kintner

(*Cornell University*, *Ithaca*, *NY*, *USA*)

Ionospheric plasma irregularities or bubbles, that are regions with depleted density, are generated at the magnetic equator after sunset due to plasma instabilities, and as they move upward they map along the magnetic field lines to low latitudes. To analyse the temporal and spatial evolution of the bubbles over Brazilian territory, the mapping of ionospheric plasma bubbles for the night of 17/18 March 2002 was generated using data collected from one GPS receiver array, and applying interpolation techniques. The impact on the performance of Global Navigation Satellites System (GNSS) and on the Space Based Augmentation System (SBAS) in the tropical regions of the GPS signal losses of lock and of the signal amplitude fades during ionospheric irregularities is presented.

KEY WORDS

1. SBAS. 2. Plasma bubbles. 3. Ionospheric irregularities. 4. GPS.

1. INTRODUCTION. Several studies have demonstrated that the equatorial ionospheric scintillations affect the performance of GPS receivers (Kintner, 2001; Bandyopadhayay et al., 1997) and create difficulties to SBAS implementation (Klobuchar et al., 2002). Ionospheric irregularities, as plasma bubbles, are determinant factors to cause scintillation. Scintillation occurs when a radio wave crosses the ionosphere and suffers a distortion of phase and amplitude. Scintillation in the signal amplitude and phase contribute to the loss of lock on GPS receivers, decreasing the number of available satellites and consequently reduces the possibility to get good satellite geometry and the necessary accuracy to meet aerial navigation requirements. Loss of lock occurs when a receiver is stressed by two factors. The first factor is rapid phase variations causing a Doppler shift in the GPS signal which may exceed the bandwidth of phase lock loop (PLL), resulting in a loss of phase lock (Leick, 1995; Skone et al., 2001). The receiver bandwidth is narrow to eliminate excess noise, however the receiver becomes more susceptible to phase scintillations. The second factor is rapid amplitude fluctuations in which the signal amplitude becomes too small to be sensed by the loop discriminator (Humphreys et al., 2005; Kintner et al., 2005). The question of which loss of lock cause is dominant is likely

to be receiver dependent and continues to be a subject of investigation. The plasma bubbles are generated in the equatorial region and maps along the magnetic field lines to low latitudes reaching the Equatorial Ionospheric Anomaly (EIA) crests, where they present larger amplitudes. The EIA, or Appleton Anomaly, consists of the formation of ionospheric regions of high electronic density (crests) that are observed around 20 degrees north and south of the magnetic latitude. It is generated during day and intensifies after sunset, in the magnetic equator. The equatorial ionospheric plasma is lifted up during daylight and it has this upward movement intensified after sunset up to 21:00 hours local time, and the plasma diffuses to low latitudes along the magnetic field lines due to pressure gradients and gravity action. This phenomenon is called Fountain Effect. Plasma bubbles generated in the equator (over São Luís), take around one hour to arrive in the EIA crest (around 20 degrees latitude). After the bubble-growing phase they normally move to the east with a velocity of about 150 m/s during the pre-midnight local time sector and this velocity decreases after midnight. Bubble occurrences are related to magnetic and solar activity (solar cycle), time of day, season and location. In Brazil, the bubbles occur from September to March, between 18:00 hours to midnight local time and in the post-midnight sector during some magnetic storms (de Paula et al., 2006).

2. METHODOLOGY

2.1. *GPS Receivers*. The receiver used to monitor ionospheric scintillation (SCINTMON) was the GEC-Plessey GPS card developed by Cornell University (Beach and Kintner, 2001) with modified software to acquire data at 50 Hz sampling rate in a single frequency L1 (1,575·42 MHz) signal amplitude. This system is able to track up to 12 satellites simultaneously, however one channel is reserved for noise. The elevation mask is 10 degrees. The scintillation S_4 index (Beach, 1998; Rodrigues, 2003) is defined as the normalized variation of the signal intensity I.

$$S_4^2 = \frac{< I^2 > - < I >^2}{< I >^2} \tag{1}$$

The procedure to calculate the scintillation index is to use a low pass filter with a cutoff of 0·1 Hz to obtain the local mean values of the channel wide band power P_k and noise wide band power N_k, where k is the sample number. The true signal strength variance, $\hat{\sigma}^2$, over a one minute period is estimated by:

$$\hat{\sigma}^2 = \frac{1}{M} \sum_{k=1}^{M} (P_k - < P >_k)(P_{k-1} - < P >_{k-1}) \tag{2}$$

where $M = 3000$ is the number of samples per minute, while P_0 and $\langle P \rangle_0$ are defined to be the final power values of previous minute interval. Consecutive values of P evaluated at k and k-1 were used to eliminate the spike effect in the autocorrelation function (ACF) due to measurement noise. Further, the mean power, $\hat{S}$, over the same period is calculated by:

$$\hat{S} = \frac{1}{M} \sum_{k=1}^{M} (< P >_k - < N >_k) \tag{3}$$

Figure 1. The array of scintillation monitors over the Brazilian territory.

In this scheme the scintillation index is calculated for each minute by the following equation:

$$S_4 = \frac{\sqrt{\hat{\sigma}^2}}{\hat{S}} \tag{4}$$

The signal acquisition consists of four steps, performed in the following order: code lock, carrier lock, bit lock and subframe lock (Beach, 1998). The receiver quickly weeds out false locks by the failure of one channel to achieve subsequent carrier, bit and subframe synchronization. The array of scintillation monitors over the Brazilian territory is shown at Figure 1. There are receivers installed in Manaus, São Luís, Cuiabá, Cachoeira Paulista, São José dos Campos, Palmas and São Martinho da Serra. The geographic latitude and longitude, magnetic declination and dip latitude of these sites are provided in the Table 1. The information received is summarized for each minute and contains parameters like satellite identification (PRN), S_4 index, WBP (Wide Band Power), Doppler (Hz) displacement, number of loss of lock, receiver and satellite coordinates. These data were imported to a MySQL relational

Table 1. Coordinates of GPS receivers stations over Brazilian territory.

STATION	GEOGRAPHIC LAT – LONG (degree)		DIP LAT. (degree)	MAGNETIC DECLINATION (degree)
MANAUS – AM	3·08 S	59·97 W	5·79	13·96 W
SÃO LUIS – MA	2·33 S	44·21 W	−1·73	20·74 W
CUIABÁ – MT	15·45 S	56·07 W	−6·56	14·98 W
CACHOEIRA PAULISTA – SP	22·57 S	45·07 W	−18·12	20·54 W
SÃO JOSÉ DOS CAMPOS – SP	23·07 S	45·86 W	−18·01	20·03 W
PALMAS – PR	26·36 S	51·98 W	−17·27	15·36 W
SÃO MARTINHO DA SERRA – RS	29·28 S	53·82 W	−18·57	12·90 W

database, the periods with a $S_4 \geqslant 0{\cdot}3$ to characterize scintillation conditions were selected, and the columns TIME and POWER were extracted from the raw data and registered the fading amplitude and duration when the signal amplitude was below 30 dB. Below this level, the signal reaches a critical point with possibilities of loss of lock occurrence. Histograms of fading and loss of lock occurrences were plotted. To compute loss of lock, we consider the time gaps in the column of extracted TIME from raw files. There is an interval of approximately 0·1 s per pulse in these data. A computer program looks for gaps larger than 0·1 s in the intervals for WBP smaller than 30 dB and satellite elevation angle larger than 40 degrees. Low elevation angle increases the probability of loss of lock due to other factors, independent of ionospheric scintillation, like multipath and weak signal to noise ratio. The program records all the above described parameters in a file for further processing.

2.2. *TerraLib Technology*. To generate the bubble mapping represented by the S_4 index we used TerraLib technology, a software library for Geographic Information System (GIS) and TerraView application, that is a front-end software for geographic mapping and environmental monitoring. These programs were developed at National Institute for Space Research (INPE) by the Images Processing Department using the C++ program language. TerraLib and TerraView are freeware and open source code. This was a favourable argument to use the software. They have interface with the main Relational Data Base Management System (RDBMS) in the market. The chosen RDBMS was MySQL that is downloaded under General Public License (GPL). We extended the concept of a geographic information system and used it to generate maps of geophysical data. One of the main characteristics of the GIS is to insert and to unify in the same database, spatial information from biotic-physics environment, urban census, satellite images and GPS data (Câmara et al., 2005).

2.3. *Ionospheric pierce point*. A method was implemented, following the Object Oriented Program (OOP) that calculates the Ionospheric Pierce Point (IPP) during the data migration process to a relational MySQL database. (See Figure 2). IPP is the point where the satellite signal penetrates an ionosphere layer. It was calculated assuming that the ionosphere is a thin and spherical layer located at 350 km of altitude. Data were represented in a regular grid, where each element of the matrix is associated to a numerical value. This numerical value is the result of the S_4 index

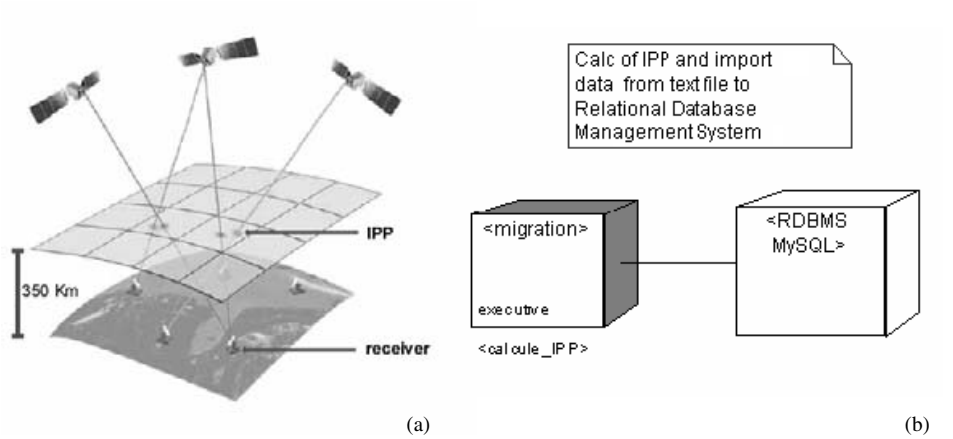

Figure 2. (a) Adapted source from Forte et al, 2002 and (b) Data migration to a RDBMS.

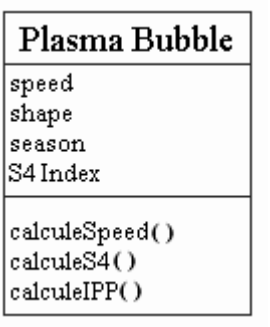

Figure 3. Modelling of a plasma bubble.

interpolation. Grids of the 5° (550 km) latitude by 5° longitude were used for Ionospheric Grid Point (IGP) at the CONUS (CONtiguous United States) region at middle latitudes (Klobuchar et al., 2002), but this grid spacing is considered insufficient to correct the ionospheric range delay in the equatorial regions where large electron density gradients are normally present. Then the grid spacing of $1{\cdot}2^\circ \times 1{\cdot}2^\circ$ (150 km × 150 km) was selected for this work. This grid is generated by the computing method of the TerraLib software.

2.4. *Bubble modelling*. Following the Unified Modelling Language (UML) and the OOP, we modelled the plasma bubble like one example of an object from bubble class (see Figure 3). Thus, we can define the attributes of the bubble as speed (about 150 m/s), and still the operations and services of this class like S_4 index calculation and the speed of the bubble. Other bubble characteristics or attributes can be added. The bubbles map along magnetic field lines so they have a shape and occur from September to March, after 18:00 hours local time for durations of about 6 hours. Measurements on the speed of the bubble, made at Cachoeira Paulista, showed that the apparent eastward velocity varies from 200 m/s to 150 m/s at 20:00 local time, and decreases to 100–50 m/s at midnight (Kil et al., 2000). The bubbles can reach the

height of 1400 km in the equatorial region. The ionospheric irregularities detected by the GPS L1 band have scale size of about 400 m that are generated inside the large scale irregularities or bubbles. The bubble east-west size is estimated to be around 480 km. There is evidence that the small scale irregularity zonal velocities are larger than the large scale structure (bubbles) velocity (de Paula et al., 2002) that matches the environment plasma velocity.

2.5. *Interpolation methods*. The interpolation follows deterministic models of the local effects. These models are based on the First Law of Geography (Tobler, 1970): *all things are related, but nearby things are more related than distant things*. Three interpolation methods were used. The simple mean was calculated between neighbours grids, estimated mean between neighbours and estimated mean between neighbours using the distance as weight. The close neighbours samples have larger influence on the estimated value. The values were interpolated for each 10 minutes. The attribute used for interpolation is the S_4 index and it was calculated using the following equation:

$$Z_i = \frac{\sum_{j=1}^{n} w_{ij} z_j}{\sum_{j=1}^{n} w_{ij}} \tag{5}$$

where Z_i is the estimated value for any point i of the grid, z_j is the value of the S_4 index, n is the number of the neighbours closer to the grid point and w_{ij} is a weighting factor:

$$w_{ij} = \frac{1}{d_{ij}^k} \tag{6}$$

where k is the exponent of the distance, generally equal to 1 or 2, and d_{ij} is the value of the distance of the sample j up to point i of the grid.

The chosen day to process and to interpolate the data and to generate the map was March, 17, 2002 that was close to a maximum solar cycle and a period of scintillation occurrence.

A cumulative distribution function (CDF) was used to survey the amplitude behaviour during scintillations. The CDF ranges from 0 to 1 and in Equation 7, f is a probability density function for the random variable X, where X represents the fading amplitude. The associated cumulative distribution function $F(x)$ is:

$$F(x) = P(X \leqslant x) = \int_{-\infty}^{x} f(t)dt \tag{7}$$

3. EFFECTS OF IONOSPHERIC IRREGULARITIES ON SBAS.

The Satellite Based Augmentation System (SBAS) uses geostationary satellites and GNSS to provide enhanced navigation services. The SBAS element in the United States is called Wide Area Augmentation System (WAAS). SBAS should be implemented through the International Civil Aviation Organization (ICAO) that legislates over civil aviation in 187 countries. Several arguments are favourable to implantation of SBAS. We can cite the optimization of the congested airways,

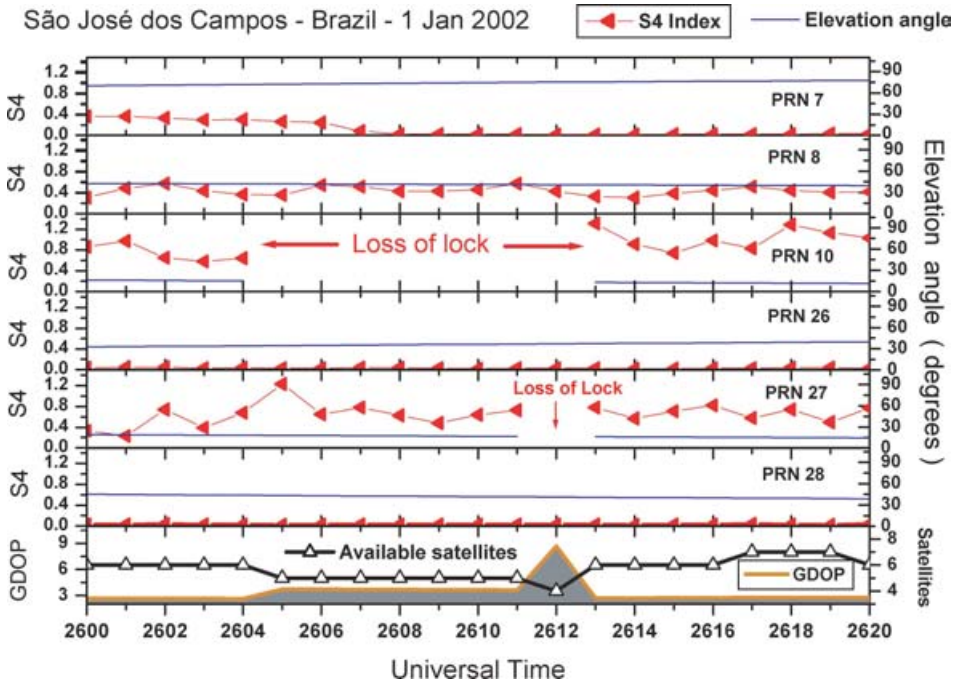

Figure 4. GDOP increases as available satellites decrease at São José dos Campos station – Jan, 1, 2002 during ionospheric irregularities.

fuel saving and the cost reduction in relation to current technology that controls air traffic. However, the implementation of SBAS has challenges in tropical regions, where the ionosphere is not as well behaved as at middle latitudes. Errors generated by ionospheric irregularities can compromise the required navigation performance (RNP): accuracy, integrity, continuity of service and availability. Accuracy is defined as the degree of conformance of an estimated or measured position at a given time to a defined reference value. Accuracy should not be confused with precision, which denotes a measurement quality that describes how well repeated measurements agree with themselves rather than with a reference value (Ochieng et al., 2003). Integrity relates to the level of trust that can be placed in the information provided by the navigation system. It includes the ability of the navigation system to provide timely and valid warnings to users when the system must not be used for the intended operation or phase of flight. Continuity of a navigation system is the capability to perform its function without non-scheduled interruptions during the intended period of operation. Availability is defined as the percentage of time during which the service is available (Ochieng et al., 2003).

When a radio wave crosses the ionosphere, it suffers a distortion of phase and amplitude. This produces amplitude and phase fluctuations that are called scintillations. Scintillations are highly dependent on the season, time of day, location, solar cycle, magnetic and solar activities. The architecture of GPS was developed in the mid-1970s and includes a code division multiple access (CDMA) protocol with a limited dynamic range, $\sim$21·6 dB (Kintner et al., 2001). The amplitude fading (called

scintillations) if deep enough and long enough, can potentially cause tracking loss. Below 30 dB C/N, the signal reaches a critical point with possibilities of loss of lock occurrence. Severe scintillations of the order 20 dB can cause loss of the signal for one or more satellites, thus potentially degrading the navigation solution (Beach et al., 2001). Amplitude scintillation fading on the GNSS satellite signals can be a serious concern for users, because this system must receive at least six GNSS satellites at all times to insure that they obtain nearly continuous ionospheric corrections from each satellite. Normally, there are from 8 to 10 GNSS satellites (on average) visible and available at any location. Four satellites are required to determine a position, velocity and receiver clock offset. A fifth satellite is required for fault detection (a satellite broadcasting faulty information) and a sixth one is required to isolate the faulty satellite (Klobuchar et al., 2002). We used scintillation data from São José dos Campos, for January, 1, 2002 to analyse the effect of the ionospheric irregularities on the GPS system. The Geometric Dilution of Precision (GDOP) was calculated. GDOP is a scalar factor based on the satellite geometry that maps the individual satellite ranging error to the error in the receiver position. Smaller values of GDOP yield more accurate receiver positions. To obtain the best navigation solution, a set of six or more available satellites is desirable. We consider GDOP $\leqslant 4$ as optimum geometry, GDOP $\geqslant 5$ and GDOP $\leqslant 8$, acceptable, and GDOP $\geqslant 9$ represents a poor geometry. Figure 4 shows one example of scintillation period when the number of satellites decreased to four, GDOP increase (>10) and the GPS satellite geometry became too poor for a navigation solution.

4. RESULTS. In the S_4 mapping over Brazil, areas with low receiver density gave numerical errors in the interpolation. So we restricted the mapping geographic longitude grid from 43° W to 63° W to make the S_4 interpolation. In the analysis only satellites with elevation angles $\geqslant 30^\circ$ were used in the IPP projection calculation. As a result of the interpolation, we could observe that the simple mean interpolation tends to produce surfaces with abrupt variations, and the estimated mean and estimated mean using the distance as weight interpolations, produced surfaces with smoothed variations. The results of the values for both methods (estimated mean and estimated mean using the distance as weight) were very similar. The difference is in the fifth decimal place. In Figure 5, we present the generation and the scattering of the bubble over Brazilian territory, here represented by the S_4 index, for some selected local times. The black dots are the IPP projection. At 18:10 local time there are no bubbles generated. However, at 20:10, one area close to the São Luís receiver, on the magnetic equator, presents a larger S_4 index (0·2) than other areas. By sequence, we can see that scintillations scatter in direction to low latitudes. The scattering is gradual and progressive, varying the colours from dark blue to green and reaching orange, when the S_4 index has values between 0·77 and 0·86 around 20:40 and red with S_4 values reaching 1·03 to 1·12 around 20:50. Between 21:00 and 21:10 there is a clear eastward movement, relative to the ground, of the bubble represented by its dark yellow signature that covers an extensive north-south area over the Brazilian territory. Around 2450 the S_4 index decreases. As the terminator (day/night boundary) moves to west and bubbles are generated after sunset there is an apparent westward movement of the bubbles.

The scintillation occurs in the equatorial region and also under the equatorial anomaly. However, under the equatorial anomaly, the scintillation is stronger than in the equatorial region. The most intense scintillation occurs near the crest of the equatorial anomaly, whereas near the magnetic equator, scintillation is normally weak to moderate (Bandyopadhayay et al., 1997, de Paula, 2003). For a magnetically quiet day (March, 17, 2002), Figure 6 shows the signal amplitude Cumulative Distribution Function and Table 2 shows that the maximum amplitude of the GPS signal during periods of scintillation in São José dos Campos under the EIA crest reaches 46·8 dB, while in São Luís, in the equatorial region, this parameter reaches 38·7 dB.

The amplitude CDF was also processed for another magnetically quiet day on December 6, 2001, during the period of the maximum solar cycle and strong scintillations (Figure 7). The largest amplitudes ranges and STD (standard deviation) were observed for São José dos Campos (under the anomaly crest) and the smallest amplitudes were observed for São Luís (see Table 3), positioned under the magnetic equator. In Cuiabá, amplitude STD and CDF were intermediate between São Luís and São José dos Campos (de Rezende et al., 2004).

Figure 8 shows the distribution of the losses of lock in function of the signal WBP (for WBP $<$ 30 db) during December, 2001, for São José dos Campos, under the anomaly peak. Only data with satellite elevation angle $>40^\circ$ were considered. There are 446 cases of the loss of lock in this month and there were a larger number of losses between 23 and 24 dB amplitude (99 cases). No loss of lock was observed for the São Luís station with elevation angle larger than 40° in December 2001. If signals fade to less than 25 dB for a particular satellite, the next combination for GDOP excludes this satellite (Bandyopadhayay et al., 2001).

5. CONCLUSIONS: We have shown in Figure 5 the generation and evolution of the plasma bubbles over Brazilian territory. The mapping shows the time development of the bubbles scattering up to low latitudes. Figure 5 shows that the tilted bubbles are a coherent factor, since the bubbles accompany the declination of the magnetic axis. The decrease of the S_4 index around 24:50 local time, is in agreement with the period of bubble duration i.e. approximately from 18:00 to 24:00 local time. More GPS receivers had been recently installed in Brazilian territory in addition to those shown in Figure 1. A larger number of GPS receivers should give a better resolution for data interpolation. In the near future new bubbles evolution maps will be processed including these extra stations. Our observations have shown that amplitude ranges of scintillation increase from the equator to the anomaly crest due to the background ionization enhancement (Sobral et al., 1980, de Paula et al., 2003). Figure 6 shows this behaviour and the characteristics are confirmed in Figure 7 by the CDF plots for December 6, 2001 and March 17, 2002. The larger amplitudes explain why no loss of lock was observed for São Luís station with elevation angle larger than 40° in December 2001. In São Luís the amplitude had a maximum amplitude of 40·3, minimum amplitude of 33·3 dB and standard deviation of 1·39 dB, while São José dos Campos had 48·1 dB, 19·1 dB and 2·89 dB for maximum amplitude, minimum amplitude and standard deviation respectively. The receiver installed in São José dos Campos had larger scintillation amplitudes than São Luís.

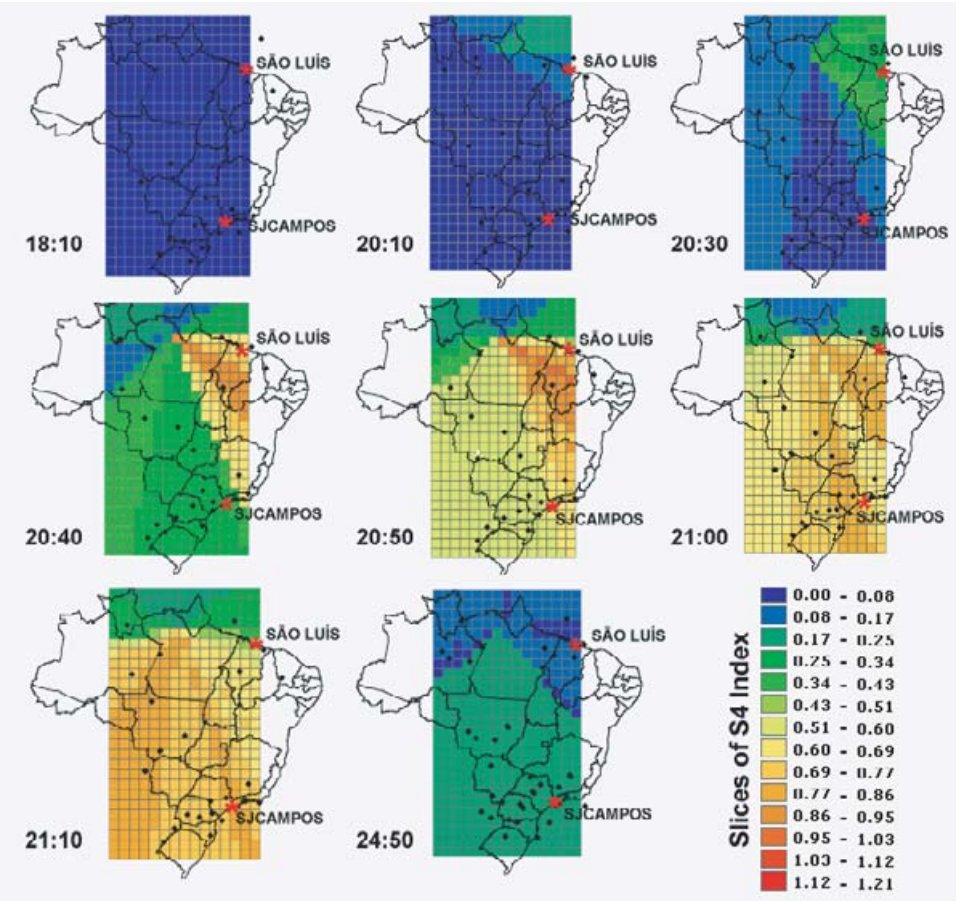

Figure 5. S_4 scintillation indices time and spatial evolution over Brazil for the night of March 17/18, 2002.

REFERENCES

Bandyopadhayay, T., A. Guha, A. DasGupta, P. Banerjee, A. Bose, (1997). "Degradation of navigational accuracy with global positioning system during periods of scintillation at equatorial latitudes", *Electronics Letters*, **33**, 12.

Beach, T. L., (1998). Global positioning studies of equatorial scintillations. PhD Dissertation, Cornell University, Ithaca, NY, USA.

Beach, T. L., P. M. Kintner, (2001). "Development and Use of a GPS Ionospheric Scintillation Monitor", *IEEE Transactions on Geoscience and Remote Sensing*, **39**, 5.

Booch, G., J. Rumbaugh, I. Jacobson, (1998). "The Unified Modeling Language User Guide (Hardcover)", Addison-Wesley Professional.

Câmara, G., (2005). "Representação computacional de dados geográficos" in "Banco de Dados Geográficos", Editora MundoGEO.

de Paula, E. R., I. J. Kantor, J. H. A. Sobral, H. Takahashi, D. C. Santana, D. Gobbi, A. F. de Medeiros, L. A. T. Limiro, H. Kil, P. M. Kintner, M. J. Taylor, (2002). "Ionospheric irregularity zonal velocities over Cachoeira Paulista", *Journal of Atmospheric and Solar-Terrestrial Physics*, 1511–1516.

de Paula, E. R., F. S. Rodrigues, K. N. Iyer, I. J. Kantor, M. A. Abdu, P. M. Kintner, B. M. Ledvina, H. Kil, (2003). Equatorial anomaly effects on GPS scintillations in Brazil, *Adv. Space Research*, **31** (**3**), 749–754.

Table 2. Maximum (MAX), minimum (MIN), mean (MEA), median (MED) and standard deviation signal amplitude for São Luís and São José dos Campos during March 17, 2002.

STATION	MAX	MIN	MEA	MED	STD
São Luís	38·7	21·9	32·4	32·9	2·64
São José dos Campos	46·8	22·5	37·3	37·8	3·08

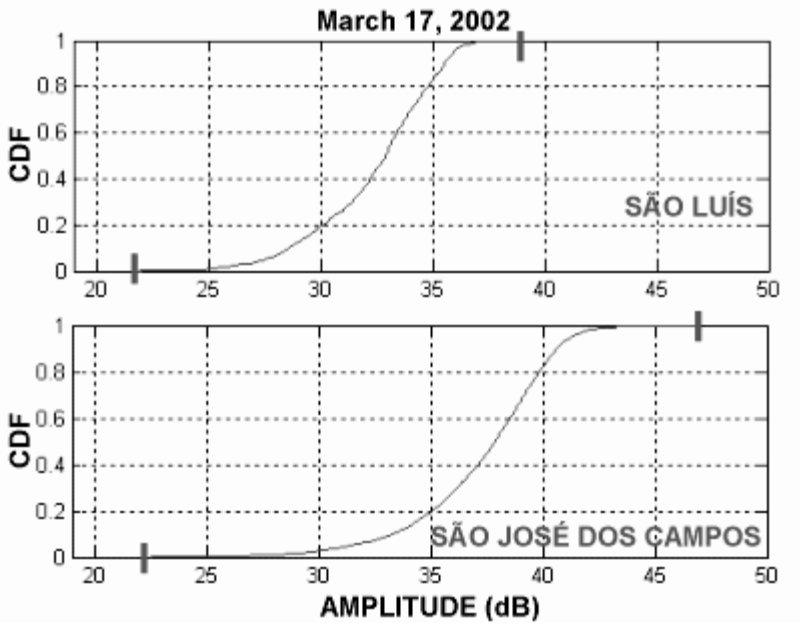

Figure 6. Cumulative Distribution Function of Amplitude for March 17, 2002.

de Paula, E. R., E. A. Kherani, M. A. Abdu, I. S. Batista, J. H. A. Sobral, I. J. Kantor, H. Takahashi, L. F. C. de Rezende, M. T. A. H. Muella, F. S. Rodrigues, P. M. Kintner, B. M. Ledvina, C. Mitchell and K. M. Groves, (2006). Characteristics of the ionospheric irregularities over Brazilian longitudinal sector, *Indian Journal of Radio & Space Physics*, New Delhi, in press.

de Rezende, L. F. C., E. R. de Paula, I. J. Kantor, P. M. Kintner, B. M. Ledvina, O. J. Branquinho, (2004). Study of lock loss duration and amplitude fading statistics on GPS L1 signal during ionospheric scintillation, at Beacon Satellite Symposium, Trieste, Italy.

Forte, B., S. M. Radicella, R. G. Ezquer, (2002). ''A different approach to the analysis of GPS scintillation data'', *Annals of Geophysics*, **45**, 3/4.

Humphreys, T. E., B. M. Ledvina, M. L. Psiaki, A. P. Cerruti, and P. M. Kintner, (2005). Analysis of ionospheric scintillations using wideband GPS L1 C/A signal data, Institute of Navigation GNSS, Long Beach, CA.

Kil, H., P. M. Kintner, E. R. de Paula, I. J. Kantor, (2000). ''Global Positioning System measurements of the ionospheric apparent velocity at Cachoeira Paulista in Brasil'', *Journal of Geophysical Research*, **105**, 5317–5327.

Kintner, P. M., H. Kil, T. L. Beach, E. R. de Paula, (2001). Fading timescales associated with GPS signal and potential consequences, *Radio Science*, **36** (**4**), 731–743.

Kintner, P. M., B. M. Ledvina, E. R. de Paula, (2005). An amplitude scintillation test pattern for evaluating GPS receiver performance, *Space Weather*, **3** (**3**), S03002, doi:10.1029/2003SW000025.

Klobuchar, J. A., P. H. Doherty, M. B. El-Arini, R. Lejeune, T. Dehel, E. R. de Paula, F. S. Rodrigues, (2002). ''Ionospheric Issues for a SBAS in the Equatorial Region'', IES2002.

Table 3. Maximum (MAX), minimum (MIN), mean (MEA), median (MED) and standard deviation signal amplitude for São Luís and São José dos Campos during December 6, 2001.

STATION	MAX	MIN	MEA	MED	STD
São Luís	40·3	33·3	36·7	36·5	1·39
Cuiabá	43·5	23·7	37·9	38·0	1·73
São José dos Campos	48·1	19·1	38·3	38·7	2·89

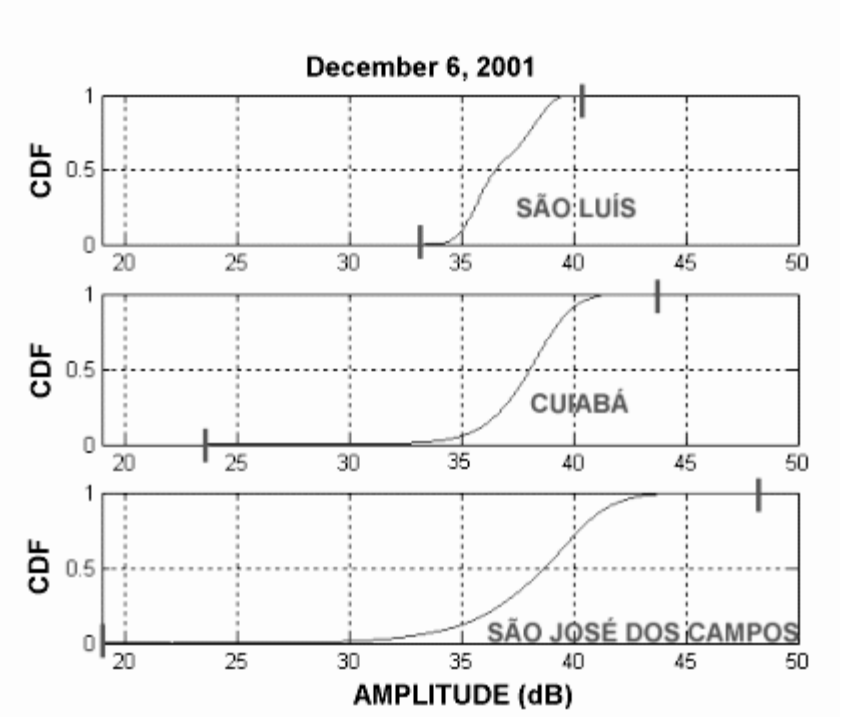

Figure 7. Cumulative Distribution Function of amplitude for Dec 6, 2001.

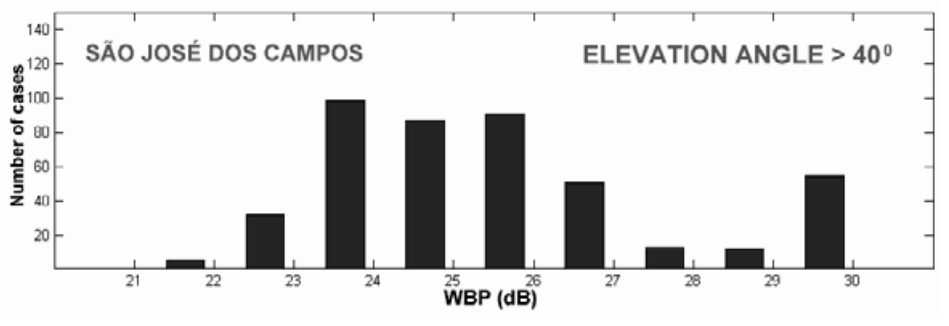

Figure 8. Number of loss of lock with amplitude less than 30 dB during December 2001.

Leick, A., ''GPS Satellite Surveying'', (1995). Second edition, John Wiley and Sons, USA.

Ochieng, W. Y., K. Sauer, D. Walsh, G. Brodin, S. Griffin, M. Denney, (2003). ''GPS Integrity and Potential Impact on Aviation Safety'', *The Journal of Navigation*, **56**, 51–65.

Rodrigues, F. S., (2003). Estudo das Irregularidades Ionosféricas Equatoriais Utilizando Sinais GPS, Msc Dissertation, INPE, Brazil.

Skone, S., K. Knudsen, M. de Jong, (2001). Limitations in GPS receiver tracking performance under ionospheric scintillation conditions, *Phys. Chem. Earth* (*A*), **26**, 613–621.

Sobral, J. H. A., M. A. Abdu, I. S. Batista, (1980). Airglow studies on the ionospheric dynamics over low latitude in Brazil, *Annales Geophysicae*, **36** (2), 199–204.

Tobler, W. R., (1970). ''A computer movie simulating urban growth in the Detroit region'', *Economic Geography* **46**, 234–240.